International Journal of Innovative Research and Advanced Studies (IJIRAS)
Volume 7 Issue 4, April 2020

ISSN: 2394-4404

Petrography And Geochemistry Of Granitoid Rocks Around Fiditi, Southwestern Nigeria: Implications For Their Petrogenesis And Tectonic Setting

Roland Anthony Isibor

Joseph Ayofe Aderogbin

Department of Earth Sciences, Faculty of Natural Sciences, Ajayi Crowther University, Oyo, Oyo State, Nigeria

Abstract: ***In an attempt to classify, decipher the petrogenesis and determine the tectonic environment of formation of the granitoids in Fiditi and environs, five rock samples were obtained and analyzed for major oxides, trace and rare earth elements using the Inductively Coupled Plasma Emission Spectroscopy. Petrographic analysis showed that the rocks are fine to medium grained, and composed predominantly of quartz, microcline feldspars, plagioclase feldspars, and biotite. Analytical result of the major oxide showed that SiO_2 concentration range from 59.33% to 75.34%. Al_2O_3 range from 13.93% to 17.11%, while Fe_2O_3 (total) range from 0.48% to 8.03%. MnO range from 0.013% to 0.223%, while MgO range from 0.14% to 2.96%. CaO range from 1.38% to 5.5%, while Na_2O range from 3.42% to 4.68%. K_2O range from 2.15% to 4.96%, while TiO_2 range from 0.0061% to 0.79%, and P_2O_5 concentration range from 0.07 to 0.21%. A plot of Na_2O+K_2O against SiO_2 showed that samples R1, R2, R4 and R5 are granites, while sample R3 is diorite. The granites showed little to positive Eu anomaly, while the diorite showed negative Eu anomaly. A plot of Zr+Nb+Ce +Y versus FeO (total)/MgO, and A/CNK [Al_2O_3/(CaO + Na_2O + K_2O)] indicated an S-type granitoids. Further plot of A/NK[Al_2O_3/(Na_2O + K_2O)] versus A/CNK[Al_2O_3/(CaO + Na_2O + K_2O)] confirmed the source magma as peraluminous. An interpretation of all the tectonic discriminatory diagrams indicated a volcanic arc+syn–collisional, active continental margin settings for the S–type granitoids of Fiditi and environs.***

Keywords: Petrography, Petrogenesis, Tectonic setting, S-type granite, Fiditi.

I. INTRODUCTION

The Basement complex of south-western Nigeria is made up of various rock types, which have been classified into migmatite-gneiss-quartzite complex; metasedimentary and metavolcanic rocks (schist belt); Pan African granitoids; and Undeformed acid and basic dykes (Rahaman, 1976; Dada, 2006). The Pan African Granitoids include several petrographic group which include charnockites, and granites.

Granitoids are the most abundant rock types in the continental crust. However, granite classification poses some difficulty because of the varieties of ways it can be formed. Granitoids can be formed from same mineral assemblage, quartz and feldspars with a variety of ferromagnesian minerals through a number of processes. Granitoids can form from differentiation of any hypersthene-normative melt and from partial melting of many rock types. Moreover, granitic melts may be derived solely from crustal components, and may form from evolved mantle-derived melts (Frost et. al., 2001).

Several classification schemes exist in an attempt to discriminate among the various petrogenetic sources and tectonic environment of formation for granitoids (Pearce et. al., 1984, Frost et. al, 2001).

Therefore, this work has applied various discriminatory geochemical plots, using major elements oxides, trace elements, and rare earth elements, in an attempt to classify,

ISSN: 2394-4404

decipher the petrogenesis and determine the tectonic environment of formation of granitoids in Fiditi and environs.

II. MATERIALS AND METHODS

A. DESCRIPTION OF THE STUDY AREA

The study area, Fiditi and environs, is geographically defined by Longitudes 3^0 55′ - 3^0 59′E and Latitudes 7^0 39′ - 7^0 45′N. This is captured on sheet 241, Oyo SE on a scale of 1:50,000 (Figure 1).

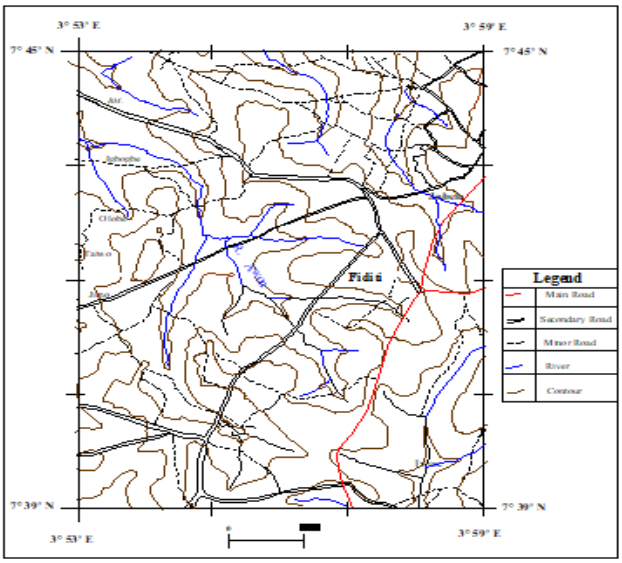

Figure 1: Topographical Map of Fiditi and Environs

It has a typical tropical climate of averagely high temperatures, high relative humidity and high rainfall. The mean temperatures are highest at the end of the Harmattan (averaging 28^0C), that is from the middle of January to the onset of the rains in the middle of March. The natural vegetation of the study area is of the tropical rainforest, and is comprised of multitudes of evergreen trees and tall grasses typical of rainforest vegetation. Factors that govern vegetation here are the climate, relief, soil type and topography and the vegetation is thicker near the rivers and streams.

The relief of the study area is generally undulating with stretches of lowlands and flood plains. In areas around Fiditi there are occurrences of rugged terrains with a lot of rocky outcrops and hills of varying altitude. The drainage pattern in the area is dendritic, showing irregular branching in all directions, with tributaries joining at all possible angles.

B. GEOLOGY OF FIDITI AND ENVIRONS

The study area, Fiditi and environs, lies within the Precambrian Basement Complex of South-western Nigeria, which is part of the Proterozoic mobile belts located between the West African and Congo Cratons (Figure 2). It lies within the region which have been subjected only to a thermos-tectonic event (Grant 1970). It has been established that the Precambrian Basement Complex of Nigeria including south-western Nigeria is polycyclic in nature, (Ajibade and Fitches 1988).

The rock suites of the basement complex have been classified as follows: Migmatite - Gneiss Quartzite Complex Suite; Metasedimentary and metavolcanic rocks (Schist Belts); Pan African Granitoids; and Undeformed acid and basic dykes (Rahaman, 1976; Dada, 2006).

The major rock types in Fiditi and environs include Banded gneiss, Granites, and Granite gneiss, with intrusions of Pegmatite. Generally, the outcrops are low lying. Banded gneiss show fairly regular and persistent alternating dark and light coloured bands. The dark band is composed dominantly of biotite and hornblende while the light band is made up of feldspars, muscovite, and quartz. The minerals commonly show well developed lineation and foliation.

Fine-to medium- grained granites were encountered quite commonly in Fiditi and environs. The granites are light coloured and composed mainly of quartz, feldspars, and biotite. The granite gneiss is a composed essentially of coarse grained feldspars and quartz. In the field, they are commonly associated with other rocks of the migmatite-gneiss complex. Structures like joints and minor folds which have subsequently been filled with granitic intrusion are quite common.

Pegmatite occur as coarse-grained veins within the crystalline rocks of the area, particularly within the banded gneiss. They are composed, essentially, of quartz, alkali feldspars and plagioclase feldspars. Their contact with host rocks may be sharp or gradational and they may be discordant or concordant.

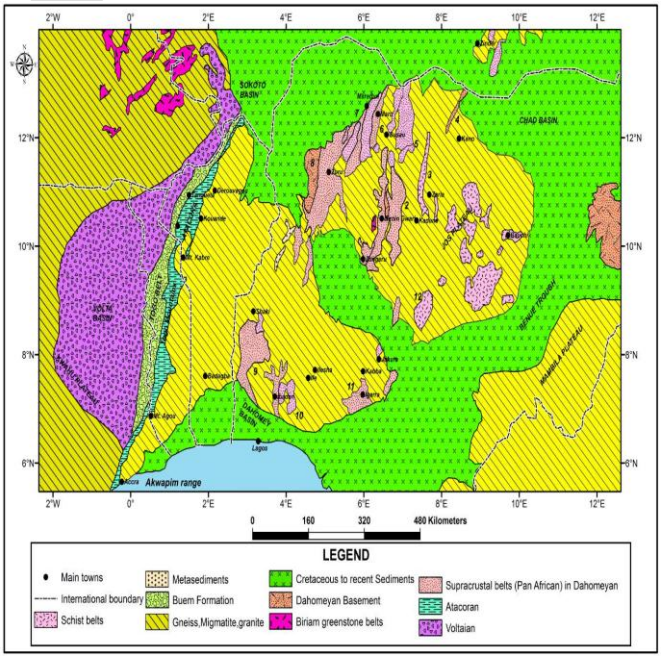

Figure 2: Basement Complex of Nigeria within the framework of the geology of West Africa (adapted from Wright, 1985)

C. FIELD SAMPLING AND PETROGRAPHIC STUDIES

Geological field mapping was undertaken in order to identify, study field occurrences and field relationships of rock types that are present in the study area. In the field, each outcrop was observed and described based on its mode of occurrence, macroscopic characteristics, structural elements and field relation with adjacent outcrops. Locations of rock samples collected were noted with the use of a Global

positioning system (GPS) and the geographic coordinates of the base map. A total of five (5) granitic rock sample were collected. Table 1 summarizes the features noted on the field.

Table 1: Field description of rock outcrops

Sample No	Coordinates	Colour	Texture	Mineralogy	Nature of Outcrop
R1	N07˚42'.25.0'', 03˚56'.01.7''E	light	Fine grained	Quartz, Potassium and Plagioclase feldspars, Biotite	Low lying
R2	N07˚39'.09.2'', 03˚55'.25.5''E	light	Medium grained	Quartz, Potassium and Plagioclase feldspars, Biotite	Low lying
R3	N07˚44'.41.1'', 03˚58'.48.4''E	light	Medium grained	Quartz, Potassium and Plagioclase feldspars, Biotite	Low lying
R4	N07˚40'.11.2'', 03˚56'.42.3''E	light	Medium grained	Quartz, Potassium and Plagioclase feldspars, Biotite	Low lying
R5	N07˚40'.24.4'', 03˚57'.09.3''E	light	Medium grained	Quartz, Potassium and Plagioclase feldspars, Biotite	Low lying

Thin section of the five rock samples were prepared at the Department of Earth Sciences laboratory, Ajayi Crowther University, Oyo and studied under the petrographic microscope for their mineral constituents and texture.

D. SAMPLE PREPARATION FOR GEOCHEMICAL ANALYSIS

Each rock is crushed in the laboratory to a nominal -2mm, mechanically split to obtain a representative sample and then pulverized to at least 95 -105 microns. The crushed rock samples were sent to Activation Laboratories, Ontario, Canada, for geochemical analysis. Sample digestion employs a lithium metaborate/tetraborate fusion technique. The resulting molten bead is rapidly digested in a weak nitric acid solution. The fusion ensures that the entire sample is dissolved. It is only with this attack that major oxides including SiO_2, refractory minerals (i.e. zircon, sphene, monazite, chromite, gahnite, etc.), REE and high field strength elements are put into solution.

E. ANALYTICAL METHODS

The sample were analyzed at the Activation Laboratory, Ontario, Canada using the Inductively Coupled Plasma Optical Emission Spectroscopy (ICP – OES) and the Inductively Couple Plasma Mass Spectroscopy (ICP – MS).

F. DATA ANALYSIS

Series of statistical and geochemical techniques were employed to analyze the data generated. The statistical analysis include descriptive statistical analysis such as range, and standard deviation. Also various discriminatory geochemical diagram were employed in order to classify the rocks, decipher their petrogenesis and determine the tectonic environment of formation (Gao, et al., 2017, Bi, et. al., 2018, Lin, et al., 2015).

III. RESULTS AND DISCUSSION

A. GEOLOGY OF FIDITI AND ITS ENVIRONS

a. PETROGRAPHICAL CHARACTERISTICS OF THE GRANITIC ROCKS AROUND FIDITI

Location 1 (R1)

The sample consists predominantly of microcline feldspar with its characteristic cross hatch twining. Microcline perthite is also evident. The plagioclase feldspar present is minute. There is an intergrowth of quartz and microcline resulting in mymekitic texture. The relative modal composition of the mineral constituent is as follows: quartz - 35.1%, microcline - 48.5%, plagioclase -8.7 %, biotite – 4.9%, and hornblende – 2.5% (Figures 3a and b).

Location 2 (R2)

The sample consists predominantly of K- feldspar. The percentage modal analysis for each of the minerals are as follows; Quartz - 29.0%, Microcline - 42.7%, Plagioclase - 15.0%, Biotite - 6.3%, and amphibole - 6.7% (Figures 4a and b).

Location 3 (R3)

The sample consists predominantly of plagioclase feldspar (Figure 5a, b and c). The relative modal count for the mineral constituent is as follows: Plagioclase: 40.8%, Quartz: 24.5%, Biotite: 19.5%, Orthoclase: 0.3%, Amphibole: 14.4%, and Augite: 0.5%.

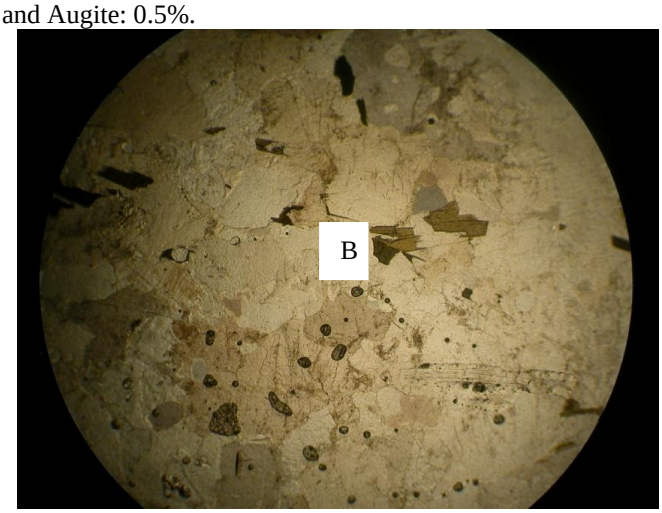

Figure 3a: Photomicrograph of a sample from Fiditi area showing specks of biotite under plane polarized light. Mag. X40

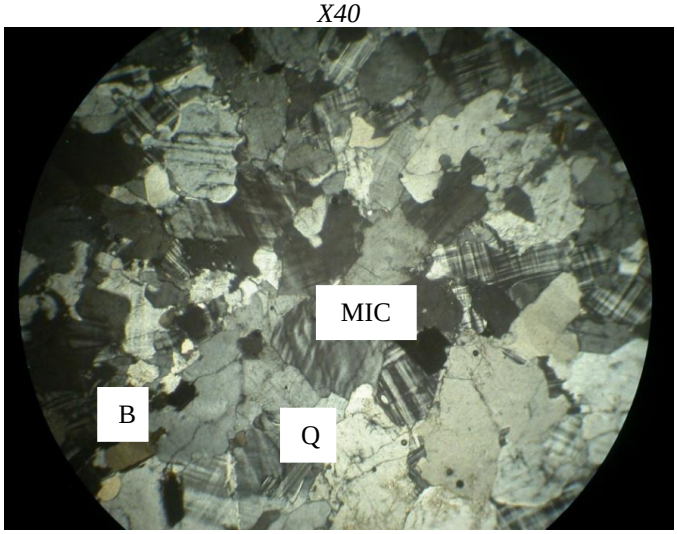

Figure 3b: Photomicrograph of a sample from Fiditi showing the microcline feldspar with its characteristic cross hatch twinning, microcline perthite, quart and biotite under cross polar. Mag. X40

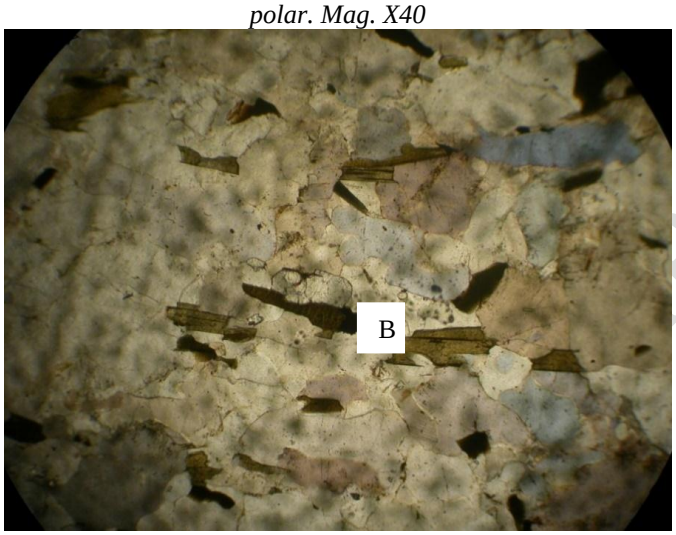

Figure 4a: Photomicrograph of sample showing biotite and quartz under ppl. Magx40

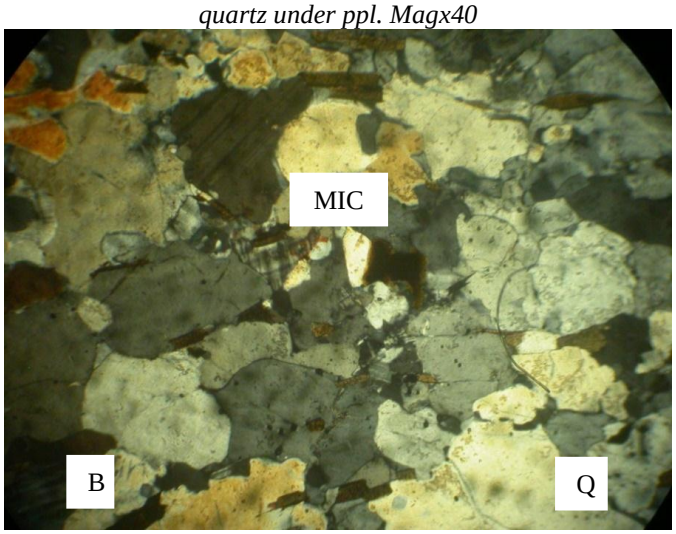

Figure 4b: Photomicrograph of sample showing quartz, microcline and biotite

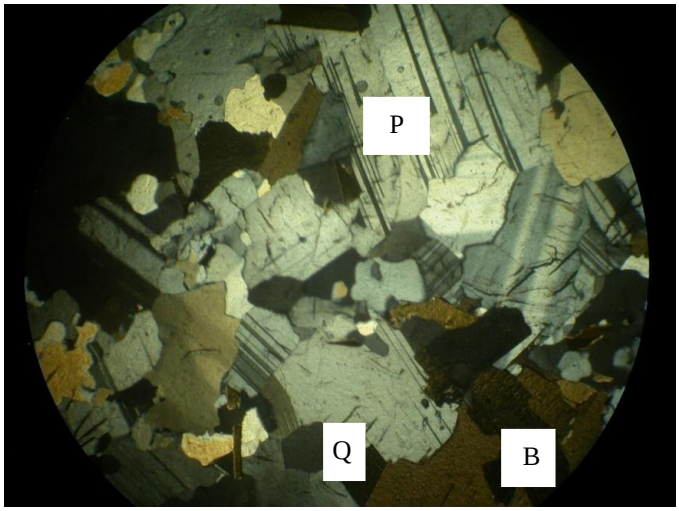

Figure 5a: Photomicrograph of sample from Fiditi area showing interlocking of plagioclase, quartz and boitite

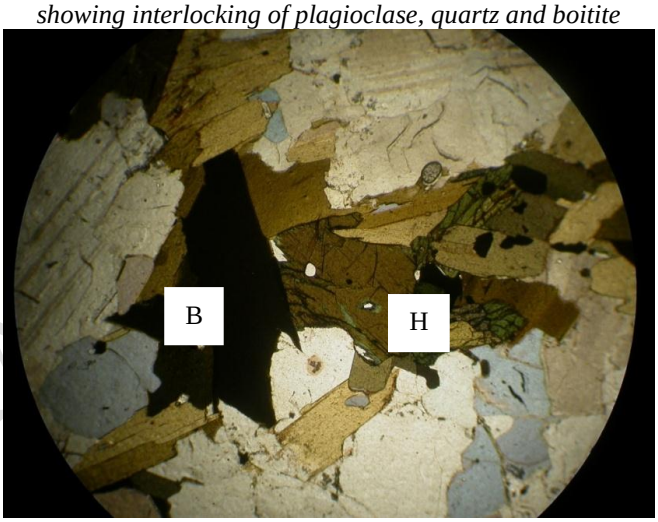

Figure 5b: Photomicrograph of sample from Fiditi area showing intterlocking of biotite and hornblende under ppl. MagX40

Location 4 (R4)

The sample consists of Quartz- 38.7%, K-Feldspar – 29.5%, Plagioclase feldspar - 26.3%, Biotite - 4.6%, Amphibole – 0.8% (Figures 6a, b and c).

Location 5 (R5)

The percentage modal analysis is as follows; - Quartz 33.1%, K- Feldspar – 32.5%, Plagioclase 20.1%, biotite 6.3%, and Amphibole 1.9%. (Figures 7a and b)

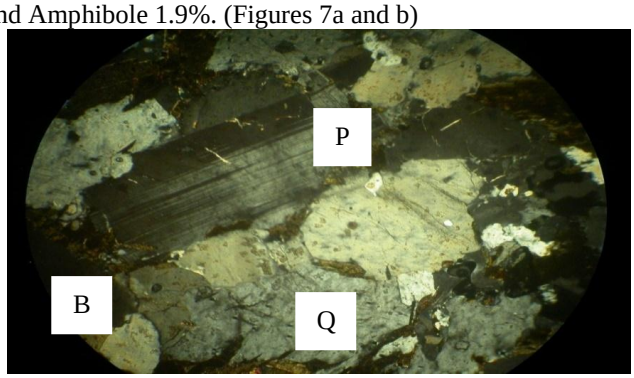

Figure 6a: Photomicrograph of a sample from Fiditi area showing coarse grain plagioclase feldspar, quart and flasks of biotite under cross polar.Mag.X40

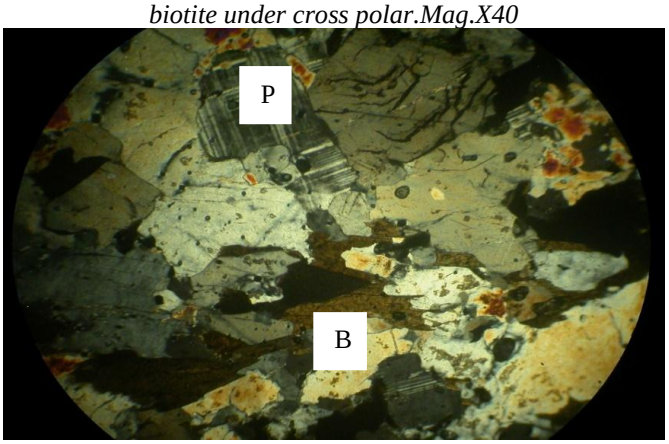

Figure 6b: Photomicrograph of a sample from Fiditi area showing, Pericline twinning in microcline, coarse grain Quartz, and Biotite. Under cross polar Mag: X 40

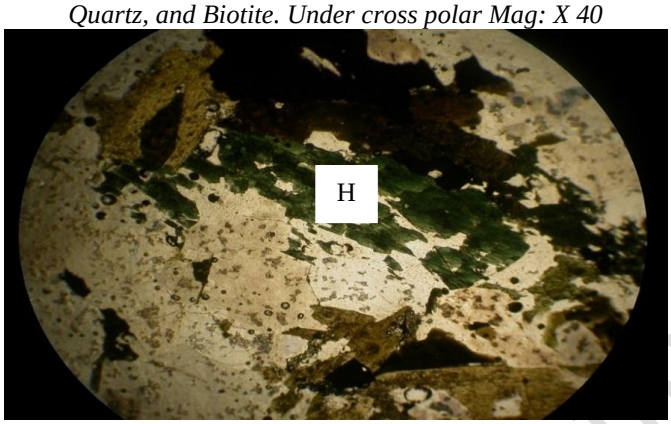

Figure 6c: Photomicrograph of a sample from Fiditi area showing the green Hornblende and brown Biotite under plane polar magnification: X40

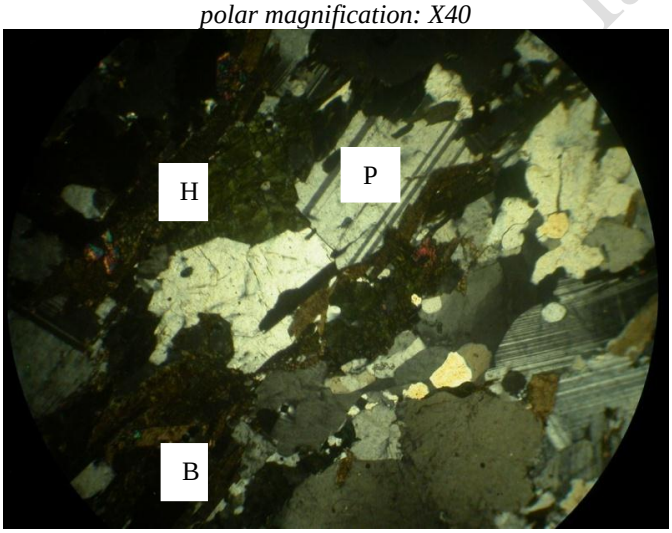

Figure 7a: Photomicrograph of sample from Fiditi area showing plagioclase, biotite, hornblende and quartz under cross polar. Mag x40

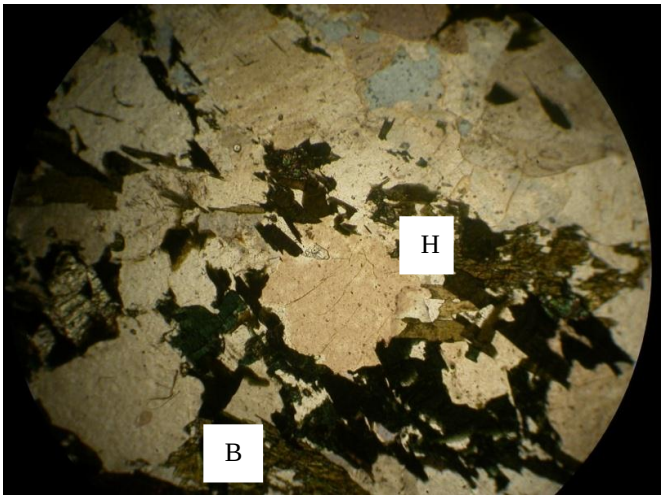

Figure 7b: Photomicrograph of Granite showing interlocking of Hornblende and Biotite flowing in a preferred direction under ppl. Mag x40

The modal analyses for the rock samples is presented in Table 2.

Table 2: Modal Analyses of the Granitic Rocks around Fiditi

Location	R1	R2	R3	R4	R5
Quartz (%)	35.1	29.0	24.5	38.7	33.1
K-Feldspar (%)	48.5	42.7	-	29.5	32.5
Plagioclase Feldspar	8.7	15.0	40.8	26.3	20.1
(%)	4.9	6.3	0.3	4.6	6.3
Biotite (%)	2.5	6.7	19.5	0.8	1.9
Amphibole (%)	-	-	14.4	-	-
Augite (%)	95	99.7	99.23	99.9	93.9
Total (%)					

B. ANALYTICAL RESULTS

a. MAJOR OXIDE

The results of the major oxides and their descriptive statistics are presented in Tables 3 and 4 respectively. The major oxides analyzed are SiO_2, Al_2O_3, Fe_2O_3 (total), MnO, MgO, CaO, Na_2O, K_2O, TiO_2 and P_2O_5. Result showed that SiO_2 range in concentration from 59.33% to 75.34%, with a mean value and standard deviation of 69.99% and 6.24 respectively. Al_2O_3 range from 13.93% to 17.11% with a mean of 15.70% and a standard deviation of 1.15, while Fe_2O_3 (total) range from 0.48% to 8.03% with a mean and standard deviation value of 2.28% and 3.23 respectively.

MnO has a mean concentration of 0.06% and range from 0.013% to 0.223% with a standard deviation of 0.09. The concentration of MgO range from 0.14% to 2.96%, with a mean and standard deviation of 0.82% and 1.20 respectively. CaO concentration range from 1.38% to 5.5%, with a mean value of 2.53% and a standard deviation value of 1.68. Na_2O concentration range from 3.42% to 4.68%, with a mean value of 4.12% and a standard deviation value of 0.59.

The concentration of K_2O range from 2.15% to 4.96%, with a mean value of 3.82% and a standard deviation of 1.10. TiO2 concentration range from 0.0061% to 0.79%, with a mean value and standard deviation of 0.29 and 0.29 respectively, while P_2O_5 concentration range from 0.07 to 0.21% with a mean value of 0.11 and standard deviation of 0.06.

Table 3: Concentration of Major Oxides in the Granitic Rocks around Fiditi and environs

Location	R1	R2	R3	R4	R5
SiO_2 (%)	71.44	75.34	59.33	70.51	73.32
Al_2O_3 (%)	16.01	13.93	17.11	15.9	15.54
Fe_2O_3 (%)	1.2	0.48	8.03	1.1	0.6
MnO (%)	0.018	0.013	0.223	0.017	0.014
MgO (%)	0.4	0.14	2.96	0.35	0.25
CaO (%)	2.09	1.38	5.5	2.02	1.67
Na_2O (%)	4.68	3.42	3.57	4.61	4.31
K_2O (%)	3.57	4.96	2.15	4.65	3.76
TiO_2 (%)	0.245	0.061	0.79	0.24	0.123
P_2O_5 (%)	0.09	0.08	0.21	0.08	0.08
LOI (%)	0.41	0.44	0.82	0.63	0.43
Total (%)	**100.15**	**100.24**	**100.69**	**100.11**	**100.10**

Table 4: Descriptive Statistics of the major elements for the granitic rocks around Fiditi and environs

	N	Minimum	Maximum	Sum	Mean	Std. Deviation
SiO_2	5	59.33	75.34	349.94	69.9880	6.23939
Al_2O_3	5	13.93	17.11	78.49	15.6980	1.14920
Fe_2O_3	5	.48	8.03	11.41	2.2820	3.22814
MnO	5	.01	.22	.29	.0570	.09282
MgO	5	.14	2.96	4.10	.8200	1.20044
CaO	5	1.38	5.50	12.66	2.5320	1.68350
Na_2O	5	3.42	4.68	20.59	4.1180	.58785
K_2O	5	2.15	4.96	19.09	3.8180	1.10040
TiO_2	5	.06	.79	1.46	.2918	.28933
P_2O_5	5	.07	.21	.53	.1060	.05857
Valid N (listwise)	5					

b. TRACE AND RARE EARTH ELEMENTS GEOCHEMISTRY

The analytical results for the trace and rare earth elements (REE) are presented in Tables 5 and 6 respectively, while a summary of the trace and REE descriptive statistics is presented in Tables 7 and 8 respectively

Table 5: Trace Element Concentration in the Granitic rocks around Fiditi and environs

Location	R1	R2	R3	R4	R5
Sc (ppm)	2	1	24	2	1
Be (ppm)	2	3	2	3	2
V (ppm)	16	<5	152	15	<5
Cr (ppm)	<20	<20	<20	<20	<20
Co (ppm)	3	1	18	2	1
Ni (ppm)	<20	<20	<20	<20	<20
Cu (ppm)	10	<10	20	10	10
Zn (ppm)	30	<30	90	30	<30
Ga (ppm)	22	20	22	21	20
Ge (ppm)	<1	1	2	1	1
As (ppm)	<5	<5	<5	<5	<5
Rb (ppm)	67	150	72	130	90
Sr (ppm)	694	215	246	543	345
Y (ppm)	4	10	40	8	6
Zr (ppm)	179	287	344	240	190
Nb (ppm)	4	2	13	3	4
Mo (ppm)	<2	<2	<2	<2	<2
Ag (ppm)	0.6	1.8	1.8	1.5	1.2
In (ppm)	<0.2	<0.2	<0.2	<0.2	<0.2
Sn (ppm)	1	24	22	10	19
Sb (ppm)	<0.5	<0.5	<0.5	<0.5	<0.5
Cs (ppm)	1	0.6	2.9	1	0.8
Ba (ppm)	1106	1033	388	1089	1042
Hf (ppm)	4.6	8	9	6	7
Ta (ppm)	0.3	0.2	0.9	0.3	0.3
W (ppm)	<1	<1	<1	<1	<1
Ti (ppm)	0.4	0.8	0.3	0.6	0.5
Pb (ppm)	18	32	8	24	28
Bi (ppm)	<0.4	<0.4	<0.4	<0.4	<0.4
Th (ppm)	7	4.9	8.1	6.2	5.6
U (ppm)	1.5	2.2	1.7	1.8	1.7

Table 6: Rare earth Element Concentration in the Granitic rocks around Fiditi and environs

Location	R1	R2	R3	R4	R5
La (ppm)	25.3	8.8	21.9	10.6	12.8
Ce (ppm)	44	16.5	59.5	20	34
Pr (ppm)	4.35	1.75	6.04	3.86	2.67
Nd (ppm)	14.6	6.2	24	12.4	8.6
Sm (ppm)	2.3	1.3	6.1	2.1	1.5
Eu (ppm)	0.61	0.69	1.48	0.67	0.65
Gd (ppm)	1.1	1.4	6.4	1.2	1.3
Tb (ppm)	0.1	0.3	1.5	0.2	0.1
Dy (ppm)	0.6	1.7	7.3	0.9	1.5
Ho (ppm)	0.1	0.3	1.5	0.2	0.1
Er (ppm)	0.3	1	4.6	0.3	0.2
Tm (ppm)	0.05	0.15	0.69	0.13	0.11
Yb (ppm)	0.2	1	4.7	0.5	0.8
Lu (ppm)	0.04	0.16	0.77	0.09	0.12
Total	**93.65**	**41.25**	**146.48**	**53.15**	**64.45**

Table 7: Descriptive Statistics of Trace Element concentration in the granitic rocks around Fiditi and environs

	N	Minimum	Maximum	Sum	Mean	Std. Deviation
Sc	5	1.00	24.00	30.00	6.0000	10.07472
Be	5	2.00	3.00	12.00	2.4000	.54772
V	5	5.00	152.00	193.00	38.6000	63.61053
Co	5	1.00	18.00	25.00	5.0000	7.31437
Cu	5	10.00	20.00	60.00	12.0000	4.47214
Zn	5	30.00	90.00	210.00	42.0000	26.83282
Ga	5	20.00	22.00	103.00	20.6000	.89443
G	5	1.00	2.00	6.00	1.2000	.44721
Rb	5	67.00	150.00	509.00	101.8000	36.59508
Sr	5	215.00	694.00	2043.00	408.6000	204.62234
Y	5	4.00	40.00	68.00	13.6000	14.92649
Zr	5	179.00	344.00	1240.00	248.0000	68.78590
Nb	5	2.00	13.00	26.00	5.2000	4.43847
Ag	5	.60	1.80	6.90	1.3800	.50200
Sn	5	1.00	24.00	76.00	15.2000	9.57601
Cs	5	.60	2.90	6.30	1.2600	.93167
Ba	5	388.00	1106.00	4658.00	931.6000	305.43461
Hf	5	4.60	9.00	34.60	6.9200	1.71231
Ta	5	.20	.90	2.00	.4000	.28284
Ti	5	.30	.80	2.60	.5200	.19235
Pb	5	8.00	32.00	110.00	22.0000	9.38083
Th	5	4.90	8.10	31.80	6.3600	1.24218
U	5	1.50	2.20	8.90	1.7800	.25884
Valid N (listwise)	5					

Table 8: Descriptive Statistics of the Rare earth elements for the granitic rocks around Fiditi and environs

	N	Minimum	Maximum	Sum	Std. Deviation
La	5	8.80	25.30	79.40	7.28814
Ce	5	16.50	59.50	174.00	17.67272
Pr	5	1.75	6.04	18.67	1.64175
Nd	5	6.20	24.00	65.80	6.88099
Sm	5	1.30	6.10	13.30	1.96672
Eu	5	.61	1.48	4.10	.37014
Gd	5	1.10	6.40	11.90	2.25765
Tb	5	.10	1.50	2.20	.59833
Dy	5	.60	7.30	12.00	2.77489
Ho	5	.10	1.50	2.20	.59833
Er	5	.20	4.60	6.40	1.88335
Ty	5	.05	.69	1.13	.26207
Yb	5	.20	4.70	7.20	1.84743
Lu	5	.04	.77	1.18	.30171
Valid N (listwise)	5				

These data were used to construct several discriminatory diagrams in order to classify the rocks, decipher their geochemical nature and determine the tectonic settings of the rocks. Furthermore, the other major oxide were plotted against SiO_2 in order to determine the trend between them (Figures 8 - 16). The plot of scatter diagram (Harker diagram) of the other major oxides against SiO_2 showed the following trend: Al_2O_3, Fe_2O_3 (total), MnO, MgO, CaO, TiO_2, and P_2O_5 concentrations decreased as SiO_2 concentration increased, while Na_2O, and K_2O concentrations increased with increasing concentration of SiO2. This trend correspond to that postulated by Bowen for the crystallization of a basaltic magma. In the plot for some trace elements Rb, Ba and Sr, showed increasing concentration as the concentration of SiO_2 increases (Figures 17 - 19), while the concentration of Zr, Ta, Th, and Nb, decreased with increasing concentration of SiO_2 (Figures 20 – 23).

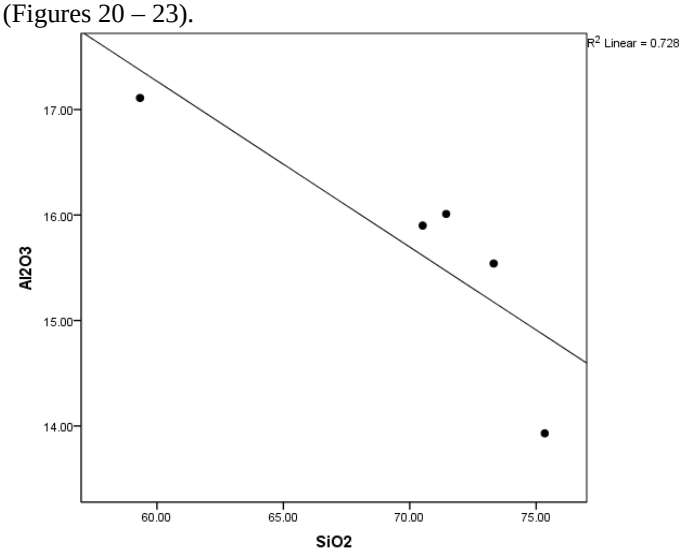

Figure 8: Scatter plot of Al_2O_3 versus SiO_2

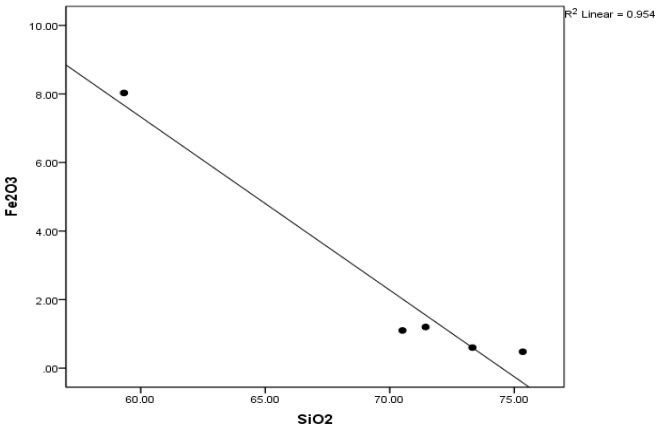

Figure 9: Scatter plot of Fe_2O_3 versus SiO_2

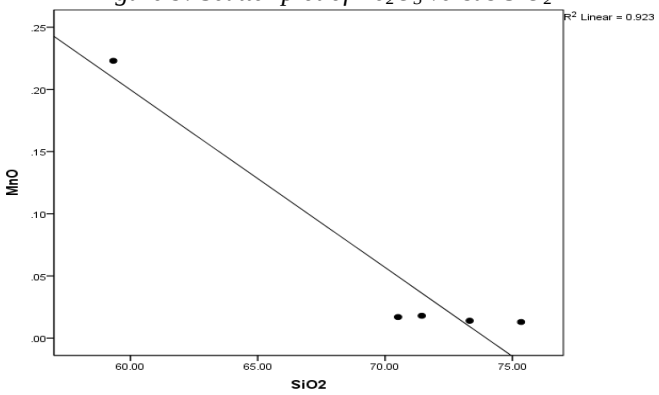

Figure 10: Scatter plot of MnO versus SiO_2

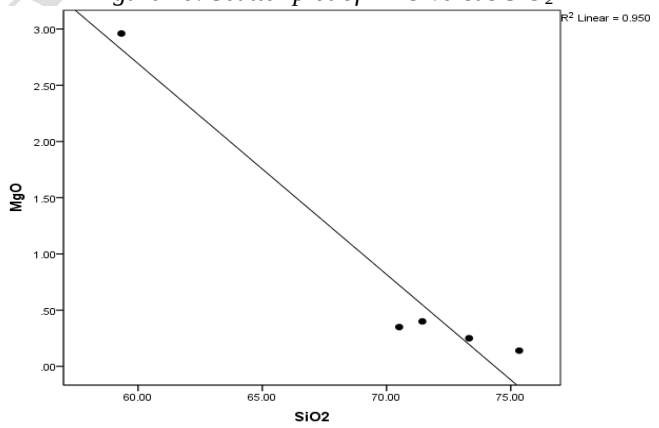

Figure 11: Scatter plot of MgO versus SiO_2

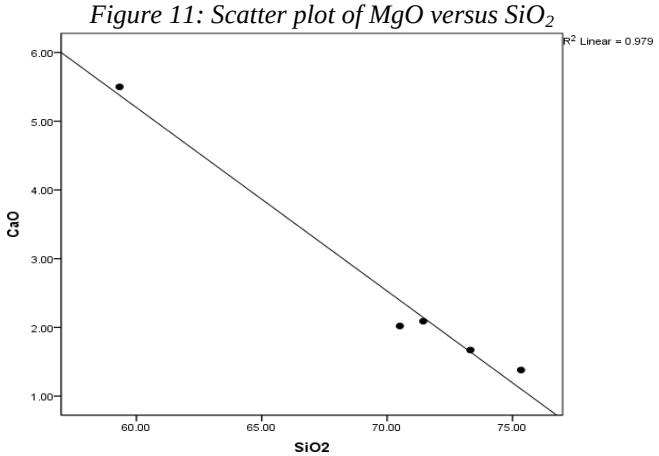

Figure 12: Scatter plot of CaO versus SiO_2

ISSN: 2394-4404

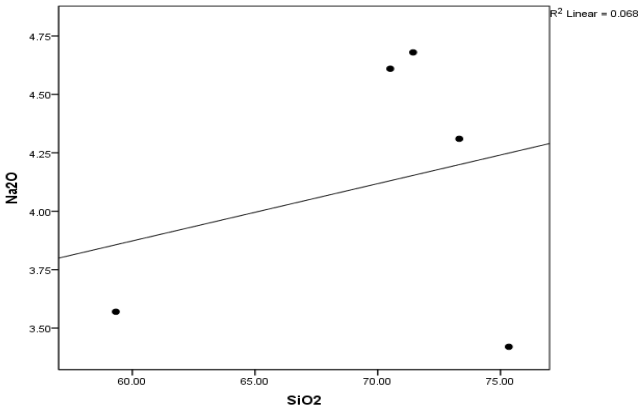

Figure 13: Scatter plot of Na_2O versus SiO_2

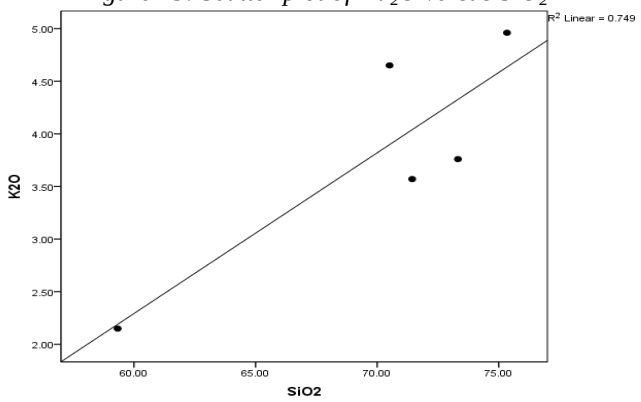

Figure 14: Scatter plot of K_2O versus SiO_2

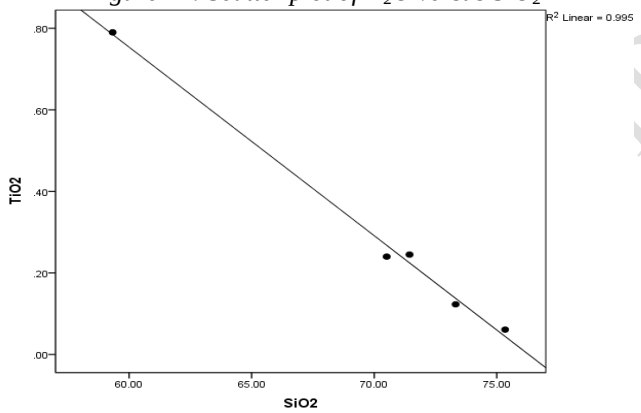

Figure 15: Scatter plot of TiO_2 versus SiO_2

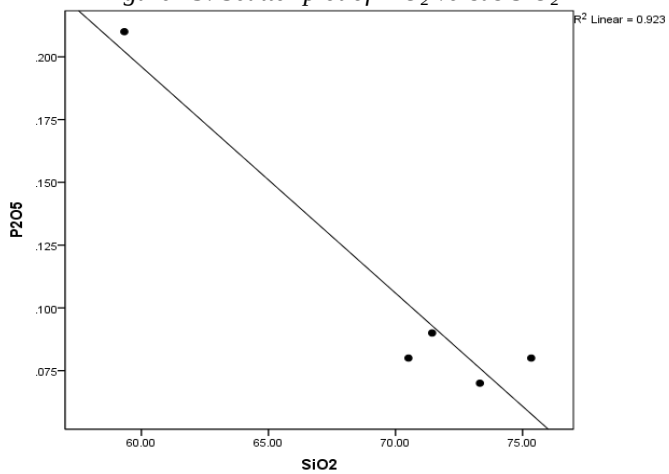

Figure 16: Scatter plot of P_2O_5 versus SiO_2

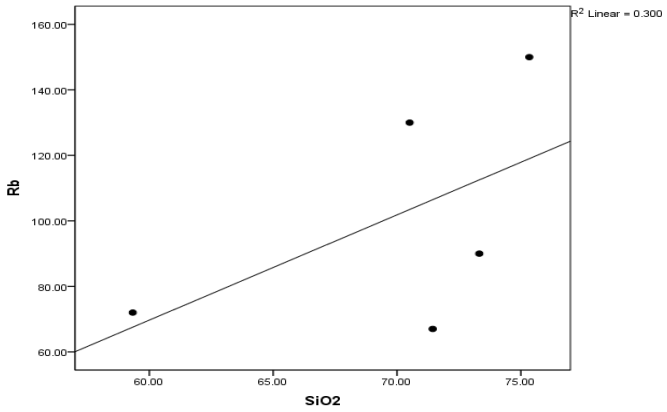

Figure 17: Scatter plot of Rb versus SiO_2

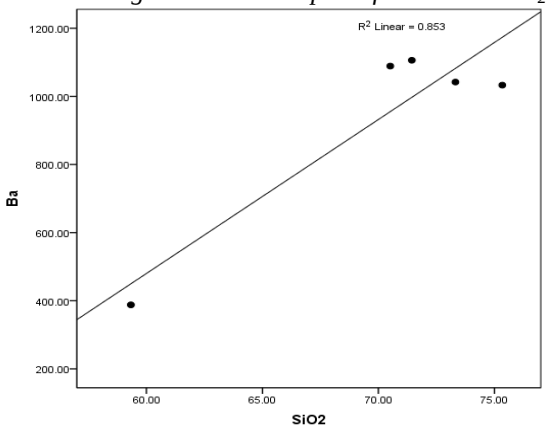

Figure 18: Scatter plot of Ba versus SiO_2

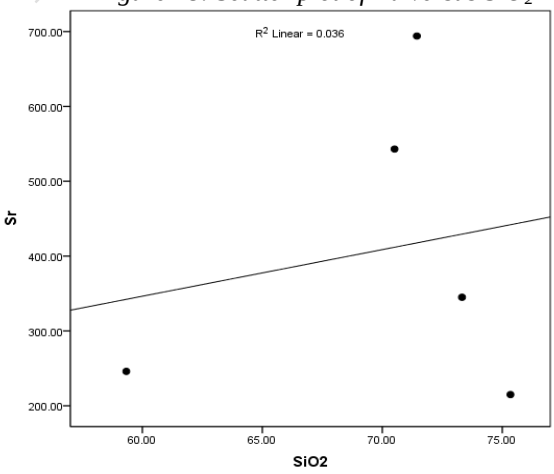

Figure 19: Scatter plot of Sr versus SiO_2

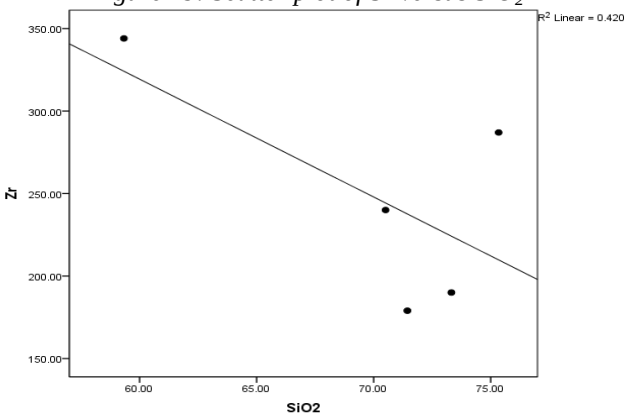

Figure 20: Scatter plot of Zr versus SiO_2

ISSN: 2394-4404

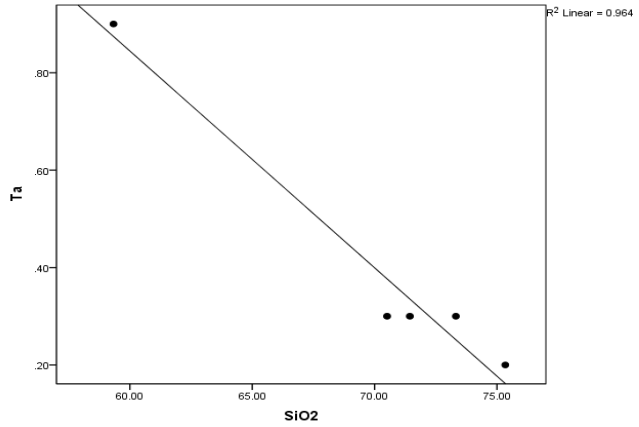

Figure 21: Scatter plot of Ta versus SiO_2

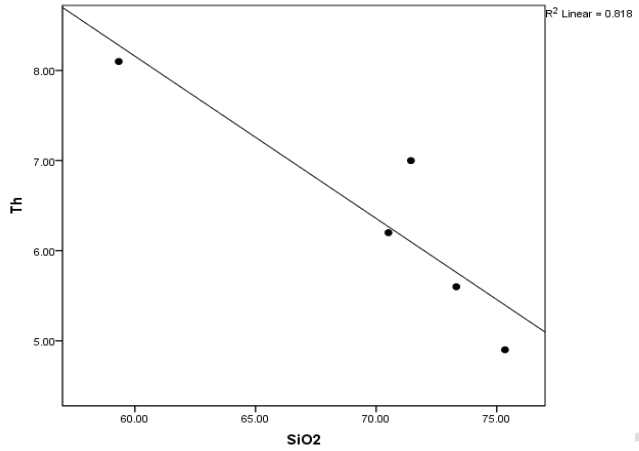

Figure 22: Scatter plot of Th versus SiO_2

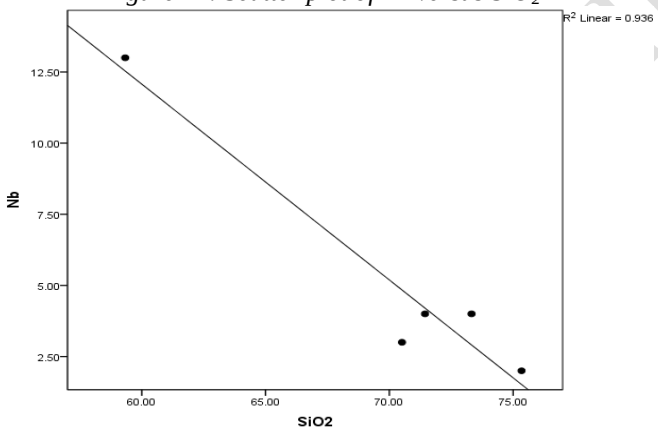

Figure 23: Scatter plot of Nb versus SiO_2

C. PETROGENETIC AFFINITY OF THE GRANITIC ROCKS

Geochemical discriminatory plots have been used to ascertain the petrogenetic affinity of crystalline rocks (Amiri et. al., 2017; Wang et. al., 2018; Zhang et al., 2018.). Based on the work of Whalen et al., 1987, Frost and Frost, 2011, Shand, 1943; Maniar and Piccoli, 1989, Peccerillo and Taylor, 1976, and Frost et al, 2001, the following discriminatory petrogenetic plots were employed to assess the petrogenetic affinity of the granitic rocks. A plot of Zr + Nb + Ce + Y versus FeO (total)/MgO (after Whalen et al., 1987) (Figure 24), put all the samples in the OTG field indicating I – S – and M – type granitoids, effectively discriminating against the A – type granitoids. A plot of Nb versus Ga/Al (after Whalen et al., 1987) (Figure 25) indicated an I and S granite rock type. A further plot of A/NK (Al_2O_3/ Na_2O + K_2O) versus A/CNK ([Al_2O_3/(CaO + Na_2O + K_2O)]) (after Shand, 1943; Maniar and Piccoli, 1989)(Figure 26) confirmed the peraluminous nature of the source magma. Furthermore, the A/CNK [Al_2O_3/(CaO + Na_2O + K_2O)], for all the samples showed values ranging from 1.41 to 1.60.

According to Raju (2008), granitoids with A/CNK values greater than 1.05 (A/CNK > 1.05) were classified as S-type granitoids. This indicate that the granitoids studied in this work are essentially S-type granites. S-type granitiods are believed to have formed from the partial melting of sedimentary and metasedimentary rocks (Raju, 2008).

A plot of K_2O versus SiO_2 (after Peccerillo and Taylor, 1976) (Figure 27), and a plot of MALI (Modified alkali-lime index) versus SiO_2 (after Frost et al, 2001) (Figure 28) indicated a high-K-calc alkaline magma source for the rock samples.

D. CLASSIFICATION OF THE GRANITOIDS

A plot of Alkali-SiO_2 of the samples showed that samples R1, R2, R4 and R5 are granites, while sample R3 is a diorite (Figure 29).

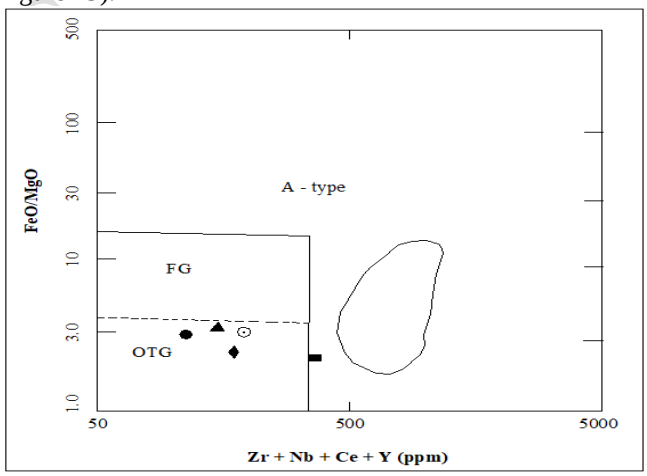

Figure 24: A plot of Zr + Nb + Ce + Y versus FeO (total)/MgO (after Whalen et al., 1987)

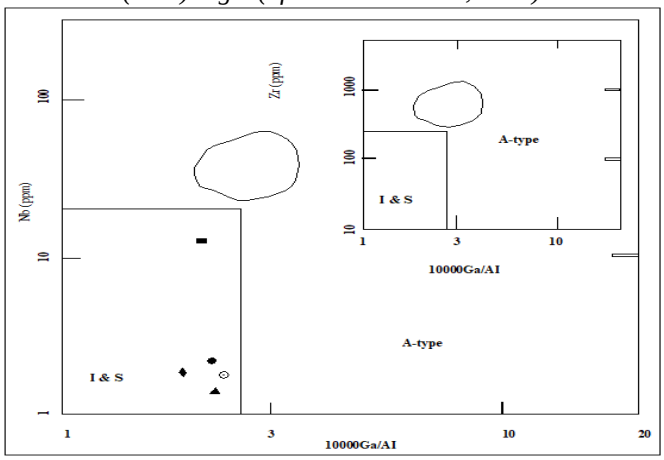

Figure 25: A plot of Nb versus G/Al (after Whalen et al., 1987)

ISSN: 2394-4404

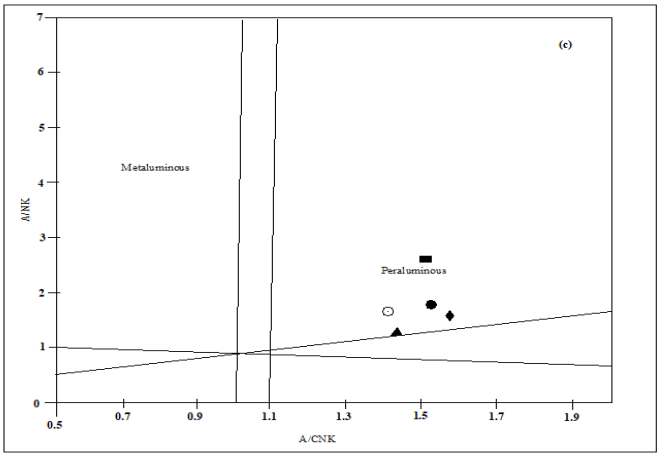

Figure 26: A plot of A/NK (Al_2O_3/ Na_2O + K_2O) versus A/CNK ([Al_2O_3/(CaO + Na_2O + K_2O)]) (after Shand, 1943; Maniar and Piccoli, 1989

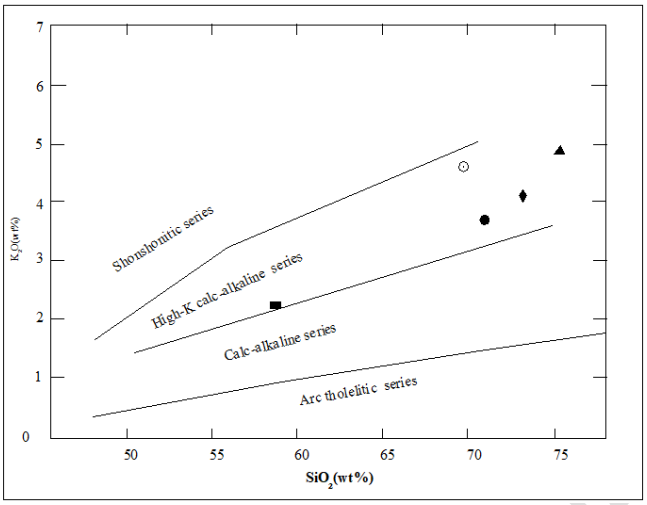

Figure 27: Plot of K_2O versus SiO_2 (after Peccerillo and Taylor, 1976)

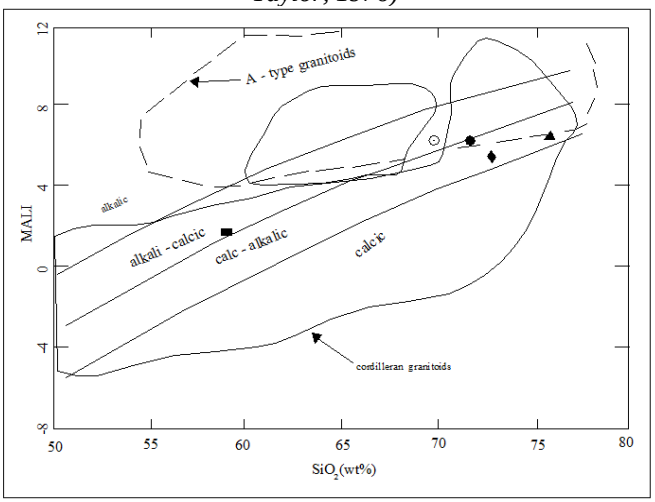

Figure 28: A plot of MALI (Modified alkali-lime index) versus SiO_2 (after Frost et al, 2001)

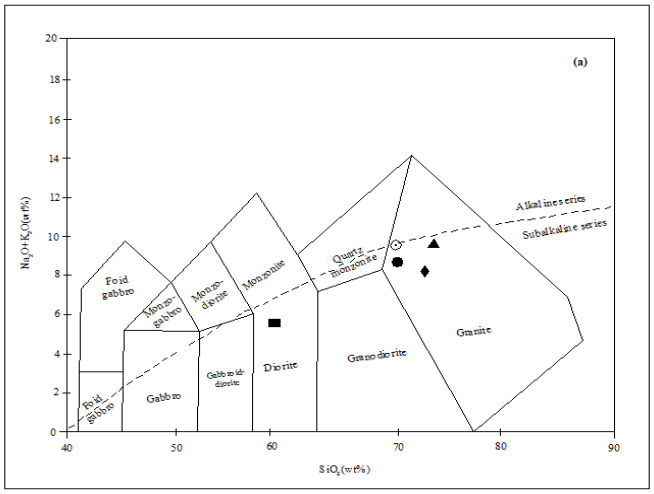

Figure 29: Alkali-SiO_2 discrimination diagram for the granitic rocks around Fiditi

E. TECTONIC SETTING

Various plots for the discrimination of tectonic settings were carried out in order to determine the tectonic environment of the formation of the rocks. A plot of Ta versus Yb tectonic discrimination diagram (after Pearce et al., 1984) (Figure 30), showed that all the granites originated in a volcanic arc setting. The trend is similar in the Nb versus Y (Figure 31) discriminatory diagram where all the samples plot in the volcanic arc + syn – collisional field, while a plot of Rb versus Ta + Yb (Figure 32) plotted in the volcanic arc granitoid field. The trend is similar for the three plots and give a volcanic arc plus a syn – collisional tectonic setting for the rock samples.

Furthermore, a plot of the rock samples on the discrimination diagrams of Th/Ta versus Yb (after Gorton and Schandl, 2000) (Figure 33), and Th versus Ta (Figure 34) indicated an Active Continental Margins environment for the granites.

A combination of the tectonic discriminatory diagram indicate a volcanic arc + syn – collisional, active continental margin settings for the granitoids. According to Raju, 2008, the typical tectonic setting for S – type granitoids is the syn – to post – tectonic continental collision setting.

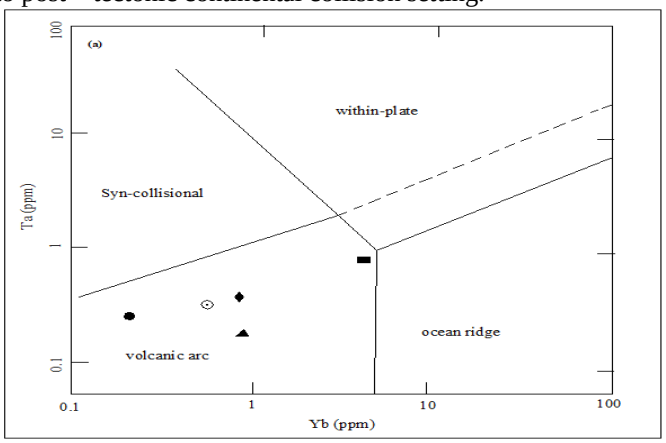

Figure 30: Ta versus Yb tectonic discrimination diagram for the granitic rocks of Fiditi and environs

ISSN: 2394-4404

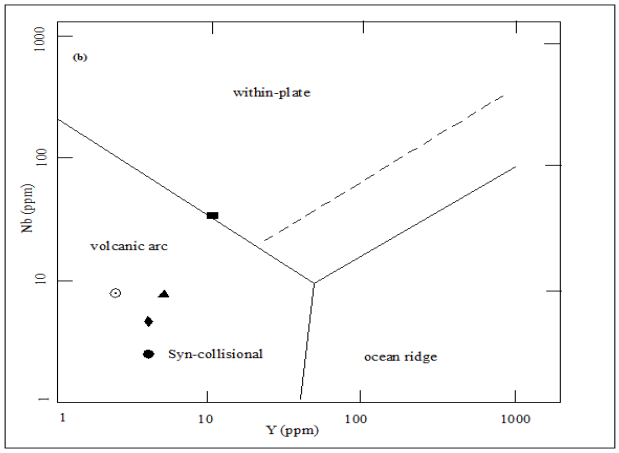

Figure 31: Nb versus Y tectonic discrimination diagram for the granitic rocks of Fiditi and environs

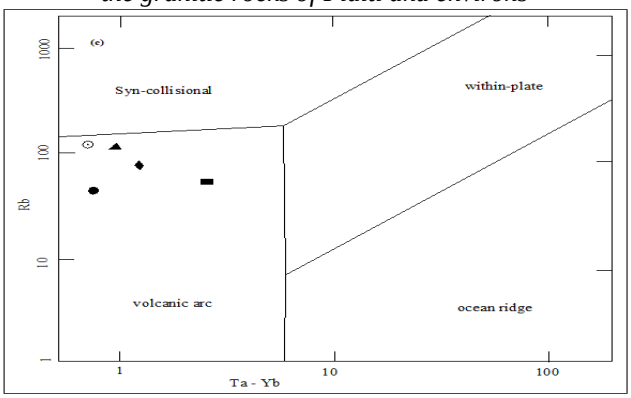

Figure 32: Rb versus Ta + Yb tectonic discrimination diagram for the granitic rocks of Fiditi and environs

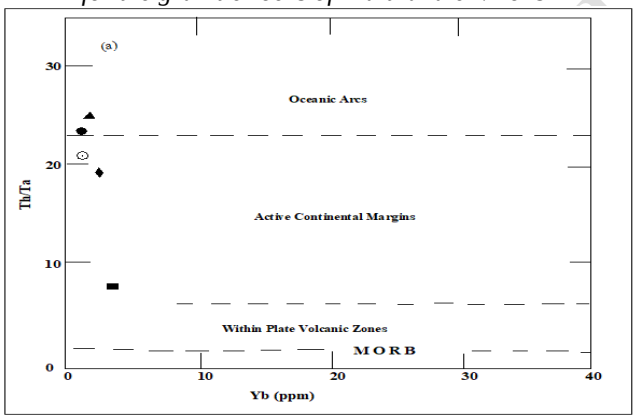

Figure 33: Th/Ta vs Yb tectonic discrimination diagram for the granitic rocks of Fiditi and environs

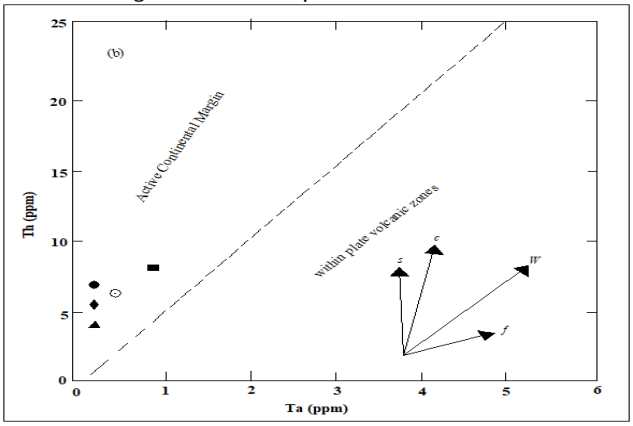

Figure 34: Th versus Ta tectonic discrimination diagram for the granitic rocks of Fiditi and environs

F. CHONDRITE NORMALIZED RARE EARTH ELEMENTS PLOTS

A plot of the chondrite normalized rare earth elements (Figure 35) indicated that the granites show little or no Eu anomaly (samples 1 and 4), to positive Eu anomaly (samples 2 and 5), while the diorite showed negative Eu anomaly, with a range of 0.27ppm to 0.53ppm for granite and 0.24ppm for diorite (Sample 3). The sum of REE content for the granite samples ranged from 41.25ppm to 93.65 ppm. This is relatively low compared to the sum of REE content for diorite of 146.48ppm.

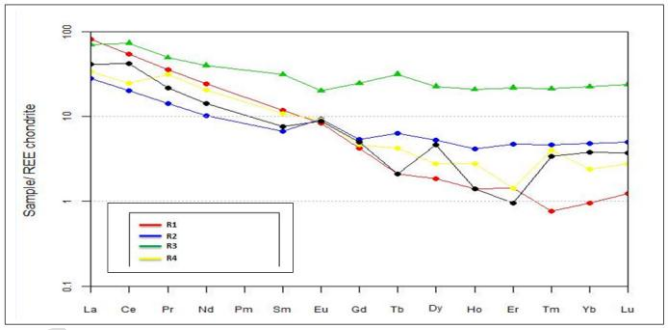

Figure 35: Chondrite normalized REE plot for the granitoids of Fiditi and environs

IV. CONCLUSIONS

The various and numerous plots of major element oxides Al_2O_3, Fe_2O_3 (total), MnO, MgO, CaO, Na_2O, K_2O, TiO_2 and P_2O_5 against SiO_2 indicated that Al_2O_3, Fe_2O_3 (total), MnO, MgO, CaO and TiO_2 concentrations decreases with increasing concentration of SiO_2, while while Na_2O, and K_2O concentrations increased with increasing concentration of SiO_2. This trend correspond to that postulated by Bowen for the crystallization of a basaltic magma. Furthermore, the plot for some trace elements Rb, Sr, showed increasing concentration as the concentration of SiO_2 increases, while the concentration of Nb, Ta and Th decreased with increasing concentration of SiO_2.

A plot of Zr + Nb + Ce + Y versus FeO (total)/MgO (after Whalen et al., 1987), put all the samples in the OTG field indicated an S-type granitoids. A further plot A/NK versus A/CNK confirmed the peraluminous nature of the source magma. Furthermore, the A/CNK [Al_2O_3/(CaO + Na_2O + K_2O)] for all the samples showed values ranging from 1.41 to 1.60 further confirming that the granites are S-type granites.

According to Raju (2008), granitoids with A/CNK values greater than 1.05 (A/CNK > 1.05) were classified as S-type granitoids. This indicate that the granitoids studied in this work are essentially S-type granites. S-type granitiods are believed to have formed from the partial melting of sedimentary and metasedimentary rocks (Raju, 2008).

A plot of K_2O versus SiO_2 and a plot of MALI (Modified alkali-lime index) versus SiO_2 indicated a high-K-calc alkaline magma source for the rock samples.

A plot of Nb versus SiO_2 showed that the granites are formed during an orogenic event. The Ta versus Yb, Nb versus Y, Ta versus Yb, Nb versus Y and Rb versus Ta + Yb tectonic discriminatory diagrams indicated a volcanic arc and volcanic arc + syncollisional tectonic environment. A furthermore plot of the rock samples on the discrimination diagrams of Th/Ta versus Yb and Th versus Ta that the granites of Fiditi and environs were formed in the Active Continental Margin.

An interpretation of all the tectonic discriminatory diagrams indicate a volcanic arc + syn – collisional, active continental margin settings for the S – type granite rock of Fiditi and environs.

REFERENCES

[1] Ajibade, A. C and Fitches, W. R. (1988). The Nigerian Precambrian and the Pan Africa Orogeny. In: Precambrian Geol Nigeria. Geological Survey of Nigeria (ed) 45–54.
[2] Amiri, M., Khalaji, A.A., Tahmasbi, Z., Santos, J.F., Sahamieh, R.Z., Zamanian, H. (2017). Geochemistry, petrogenesis and tectonic setting of the Almogholagh batholith in Sanandaj-Sirjan zone, Western iran. Jornal of African Earth Sciences.
[3] Bi, J-H., Ge, W-C., Xing, D-H., Yang, H., Dong, Y., Tian, D-X., Chen, H-J. (2018). Paleoproterozoic meta-rhyolite and meta-dacite of the Liaohe Group, Jiao-Liao-Ji Belt, North China Craton: Petrogenesis and implications for tectonic setting. Precambrian Research.
[4] Chapell, B. W., & White, A. (1974). Two Contrasting Granite Types. Pacific Geology, 8. 173-174
[5] Dada, S.S. (2006). Proterozoic Evolution of Nigeria. The Basement complex of Nigeria and its mineral resources (A tribute to Prof. M.A.O. Rahaman). Akin Jinad and Co. Ibadan. 29-44.
[6] Frost, B.R., Barnes, C. G., Collins, W. J., Arculus, R. J., Ellis, D. J., and Frost, C. D. (2001). A geochemical classification for granitic rocks. Journal of Petrology, (42): pp. 2033-2048
[7] Frost, C. and Frost, B.R. (2011). On Ferroan (A-type) Granitoids: their Compositional Variability and modes of origin. J. petrol. 52, 39 – 53.
[8] Gao, P., Zheng, Y., Zhao, Z. (2017). Triassic granites in South China: A geochemical Perspective on their characteristics, petrogenesis, and tectonic significance. Earth-Science Reviews.
[9] Grant, N.K. (1970). Geochronology of Precambrian Basement Rocks from Ibadan, southwestern Nigeria. Earth and Planetary Science Letters 10: pp. 29-38
[10] Lin, M., Peng, S., Jiang, X., Polat, A., Kusky, T., Wang, Q., Deng, H. (2015). Geochemistry, petrogenesis, and tectonic setting of Neoproterozoic mafic-ultramafic rocks from the western Jiangnan orogeny, South China. Gondwana Research.
[11] Maniar, P.D. and Piccoli, P.M. (1989). Tectonic Discrimination of granitoids. Geological society of America Bullettin. 101, 635-643.
[12] Pearce, J.A., Harris, N.B.W., Tindle, A.G. (1984). Trace element discrimination diagram for the tectonic interpretation of granitic rocks. J. Petrol., 25, 956-983.
[13] Peccerillo, A., and Taylor S.R. (1976). Geochemistry of Eocene calc-alkaline volcanic rocks from the Kastamonu area, Northern Turkey, Contributions to Mineralogy and Petrology 58, 63-81.
[14] Rahaman, M. A. (1976). Progressive polyphase metamorphism in pelitic schists around Aiyetoro, Oyo State, Nigeria. Journal of Mineralogy and Geology. 13: pp. 33-44.
[15] Raju, R.D. (2008). I-, M-,A-, and S- type Granitoids: Their attributes and mineralization, with Indian examples, 4th Prof. C. Mahadevan's Mem. Lecturer SAAEG (Indian Chapter), Kumaon Univ., Nainital, India. Jour. Eco. Geol. And Georesource Management, v.5, nos 1& 2, plp. 1-23.
[16] Shand, S.J. (1943). The Eruptive Rocks, 2nd edn. New York. John Wiley. 444p.
[17] Wang, T., Wang, D., Wang, Z., Lu, H., Wang. M., Santosh, M. (2018). Geochemical and geochronological study of early Paleozoic volcanic rocks from Lajishan accretionary complex, NW China: Petrogenesis and tectonic implications. Lithos.
[18] Whalen, J.B., Currie, K.L. and Chappel, B.W. (1987). A-type granite: Geochemical characteristics and petrogenesis. Cont. Min. Petrol., 95:407-419.
[19] Wright, J.B. (1985). Geology and mineral resources of West Africa., London: George Allen & Unwin.
[20] Zhang, X-N., Li, G-M., Qin, K-Z., Lehmann, B., Li, J-X., Zhao, J-X., Cao, M-J., Zou, X-Y. (2108). Petrogenesis and tectonic setting of Early Cretaceous granodioriric porphyry from giant Rongna porphyry Cu deposit, central Tibet. Journal of Asian Earth Sciences.